Characterization of acoustic noise and vibrations due to magnetic forces in induction machines for transport applications using MANATEE software

E.Devillers[1,2], J. Le Besnerais[1], Q. Souron[1], M. Hecquet[2]
[1] EOMYS ENGINEERING
121, rue de Chanzy, 59260 Lille Hellemmes, France, www.eomys.com
[2] L2EP, Ecole Centrale de Lille
Cité Scientifique, 59652 Villeneuve d'Asq, France
e-mail: **contact@eomys.com**

Abstract

This paper studies the effect of magnetic forces on acoustic noise and vibrations of electrical machines designed for transport applications, and more especially induction machine used for traction application. The sources of electrical noise in electrical transportation systems are first briefly reviewed. Then, the main physical phenomena responsible for acoustic noise and vibration induced by Maxwell forces in a traction induction machine are reviewed, namely slotting, winding, saturation, eccentricity, asymmetries of the magnetic circuit, and Pulse Width Modulation Effect. In this example the main resonance is due to slotting effect and a detailed analysis of the harmonics (magnetomotive force and permeance waves) is provided based on convolution properties.

All the numerical results and noise reconstitutions presented in this paper has been obtained thanks to MANATEE® software. MANATEE is a multi-physics environment dedicated to the fast design of electrical machines, including the computation of acoustic noise and vibrations due to magnetic forces, along with acoustic power level at variable speed.

1 Introduction

1.1 Noise due to electromagnetic forces in transports

Audible noise due to electromagnetic forces must be distinguished from the electromagnetic noise that concerns electromagnetic compatibility (EMC). This audible noise may be defined as the acoustic radiation due to the presence of variable electromagnetic fields in an electromagnetic circuit, such as an electrical machine. Either these fields induce directly a deflection of the circuit, as this is the case for magnetostriction, or they generate forces, such as Maxwell forces, that will induce a deflection of the circuit. The deflection propagates as vibrations to the air which may produce audible noise.

Transportation means with electrical devices naturally generate electromagnetic fields, especially devices which store, convert and dissipate electrical energy. Among them, passive and active devices have to be distinguished. Passive devices aim to adapt the electricity, which is then converted into to mechanical energy by active devices. Vibration harmonics due to passive components are related to current and voltage harmonics, while vibration harmonics due to active components are also related to the mechanical frequency (ex: revolution frequency of the shaft for electrical machines).

Passive components include static converters, filters and other circuit components:

- Rectifiers, inverters, choppers
- Capacitors, inductors

- Transformers
- Braking resistors (rheostats)
- Heating resistors
- Wires

Active devices include every electrical actuators, especially electrical machines for traction. Depending on the component type and its materials, the following equivalent forces may exist:

- Magnetostatic Maxwell forces, also called reluctance forces (ex : stator of traction machine)
- Electrostatic Maxwell forces (ex : between both sides of a capacitor)
- Magnetostrictive forces (ex : in a ferromagnetic circuit of an inductor)
- Electrostrictive forces (ex : in a dielectric elastomer)
- Lorentz forces (ex : only for a conductor in an external electromagnetic field)
- Piezoelectric forces

Identifying the sources of audible noise due to electromagnetic forces may be difficult for complex systems where the electrical devices cannot work independently, for instance electrical machines supplied by power electronics converters. Besides, some permanent electromagnetic sources such as permanent magnets in traction machines prevent from switching off all the electrical devices to verify the implication of a specific source in the overall noise.

Accurate experimental measurements coupled with knowledge in electrical engineering are often required to fully understand the origins of noise. For each involved electromagnetic forces, vibrations are either linear or quadratic dependent on voltage and current.

1.2 Noise due to magnetic forces in railway traction machines

Among the numerous electrical systems that are involved in electrical transports, this paper deals more especially with Squirrel Cage Induction Machines (SCIM, see Figure 1 Cross-sectional view of a SCIM) dedicated to railway applications. They are suited to this application thanks to their low production cost as regards on their robustness. In such machine, most of the audible noise is only due to magnetic forces at some operating points. This type of noise is often called “electrical noise” to be distinguished from EMC, but it wrongly implies a restriction to electrical fields. On the contrary, the single “magnetic noise” denomination would hide the electrical coupling that exists between electric and magnetic circuits of the machine. The denomination “electromagnetic acoustic noise” is therefore preferred.

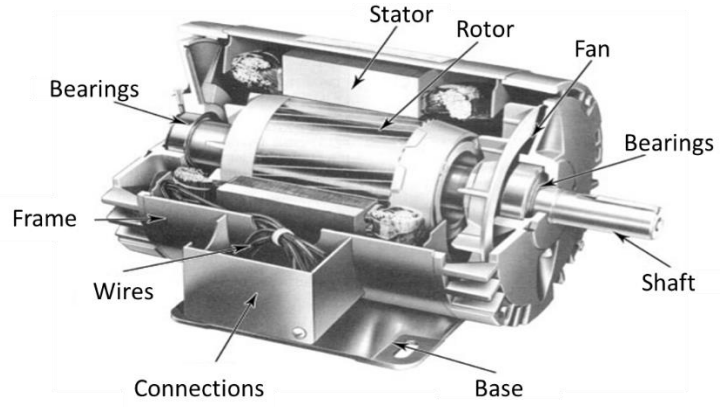

Figure 1 Cross-sectional view of a SCIM

These traction machines are often coupled with a reducer. The different pathways of noise and vibrations, including aerodynamic (ex: fans), mechanical (ex: bearings) and electromagnetic noise are illustrated on Figure 2.

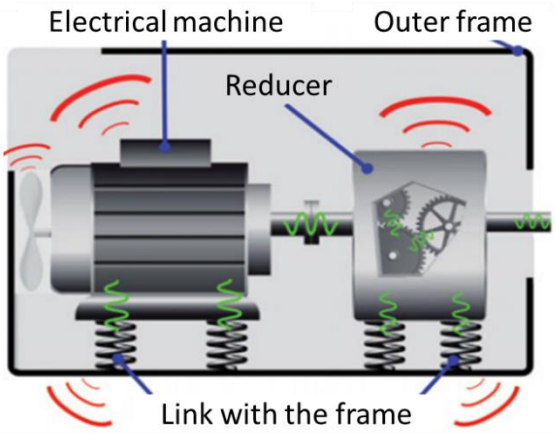

Figure 2 Pathways of noise (in red) and of vibrations (in green) in an electrical machine [1]

The aerodynamic noise generally prevails at high speed for self-ventilated machines (meaning the fan is directly mounted on the shaft) with opened frame. It is not the case for closed frame machines, or machines with external ventilations or water cooling. The mechanical noise especially due to the reducer may also be important on the whole speed range. Hence the electromagnetic noise usually predominates in railway traction machines either at low speed (effect of Pulse Width Modulation (PWM) [2]), or at medium speed [3][4] ("tooth" effect [5]).

Among all the electromagnetic forces previously presented, these can be restricted to Maxwell forces and magnetostriction when studying electrical machines. Maxwell forces are concentrated in the air gap, at the interface between the stator and the rotor, while magnetostriction acts inside stator and rotor steel sheets (Figure 3).

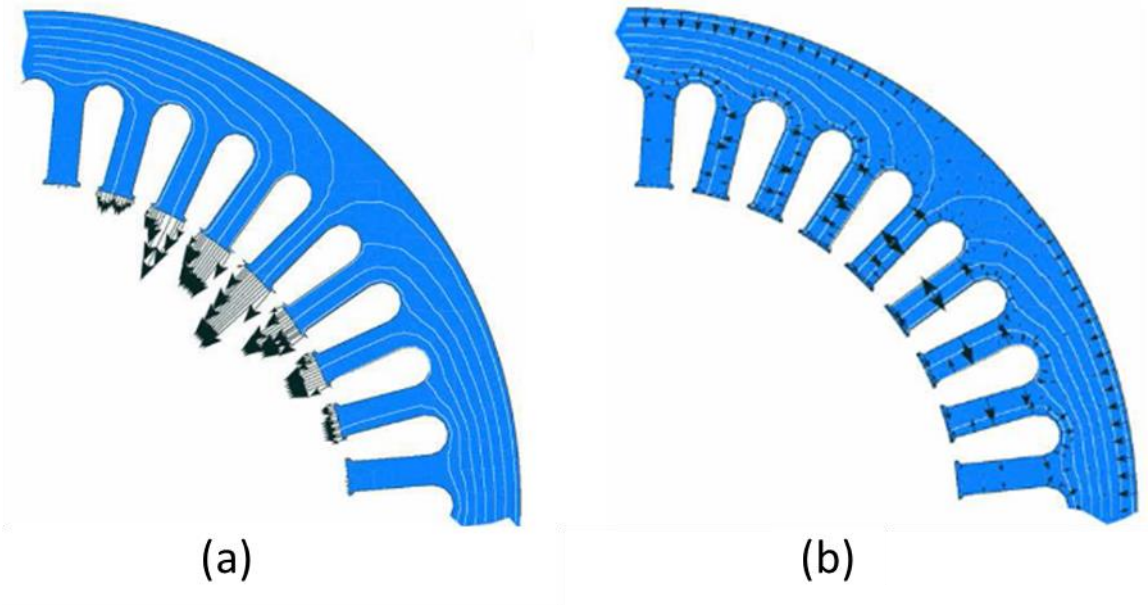

Figure 3 Electromagnetic forces acting on a SCIM stator. (a) Maxwell Forces, (b) Magnetostriction [6]

The effect of magnetostriction in terms of emitted noise is still at debate state among the scientific community, though most of the authors assume in their models that Maxwell forces remain the main cause

of noise and vibrations from electromagnetic sources in electrical machines. In fact, both type of forces are quadratic dependent on the flux density, which can explain the difficulty to dissociate them. In this paper, only Maxwell forces are considered. From the authors' experience on several dozens of machines from W to MW range, all the electromagnetic acoustic noise issues could be explained by Maxwell forces.

As shown in Figure 3, Maxwell forces are mostly radial in an induction machine, and tend to get stator and rotor closer to each other. The amplitude of the first force harmonic at twice the fundamental electrical frequency creates a pressure of around 10 tons per square meter. These pressure harmonics generate stator yoke deflection, and may resonate with one of its structural mode. The stator yoke's most important modes are the cylinder modes, which are depicted in Figure 4.

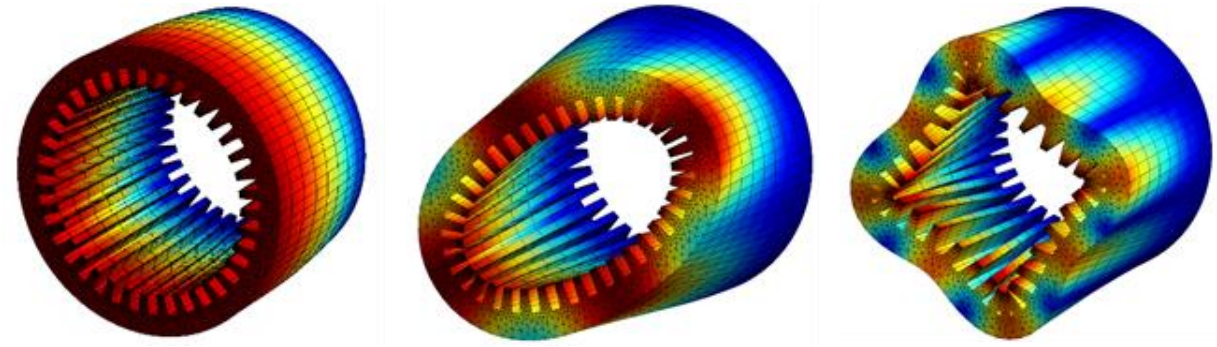

Figure 4 Examples of yoke structural mode of order (0,0), (2,0) and (4,0) obtained with MANATEE [7] (clamped/free boundary condition)

Resonances often occur in railway applications with variable speed machines supplied by PWM which introduces variable current harmonics, which induce magnetic fields. From zero speed to nominal speed, magnetic forces hence excite a large frequency band, increasing the risk of matching with a structural mode of the machine.

2 Modelling of noise due to electromagnetic forces

2.1 Introduction

Sound-insulation systems for noisy electrical machines are expensive, heavy and thermally inefficient. Besides, redesigning a manufactured machine to avoid noise due to electromagnetic forces may also be costly as electrical and mechanical properties are also coupled to electromagnetics behavior and needs to be redesigned eventually.

Consequently, the noise due to magnetic forces has to be predicted during early basic design iterations to avoid any resonances. Moreover, it is necessary to have advanced diagnosis tools for existing noisy machines to guide their redesign. To achieve such study, models using Finite Element Method (FEM) have a major drawback: the whole coupling of electromagnetic, vibration and noise models is extremely time consuming. Hence full FEM simulation is not suitable to sensitivity studies and numerical experimentation that are essential for optimization purpose. Furthermore, the multi-physics coupling (as shown in Figure 5) with FEM is rather tedious, and may not include the highest frequencies (for example ~10 kHz with PWM). It is therefore necessary to develop hybrid simulation methods.

2.2 MANATEE software

MANATEE software [7] (Magnetic Acoustic Noise Analysis Tool for Electrical Engineer) is a simulation environment dedicated to compute noise and vibrations due to electromagnetic forces of electrical machines

at variable speed. Its main specificities are the fast computation time (only few seconds for a variable speed computation up to 20 kHz), and the fully-automated multi-physics coupling in a single environment.

The MANATEE simulation process is presented in Figure 5. The electrical module first computes the Equivalent Electrical Circuit (EEC) of the machine, deducing supplying currents and voltage. Then the electromagnetic module computes the 3D time and space distribution of the magnetic flux density created by the currents. It enables to compute the resulting magnetic forces and estimate the effect on the stator yoke within the structural module. Finally, the acoustic module estimates the acoustic pressure and power level from the structure deflection.

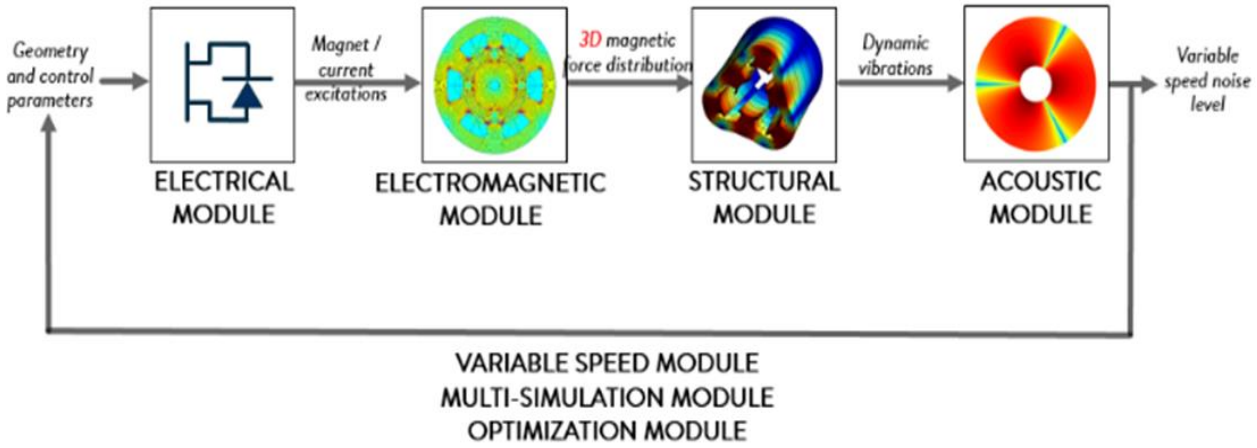

Figure 5 MANATEE simulation process

Figure 6 shows a relevant comparison between "blind" predictions from MANATEE simulations and experimental tests done on two different machines, consisting in a speed ramp from 0 to 7 krpm. In this case the simulation enables to reduce radiated noise by 40 dB. For the experimental setup, both motors are driven with PWM and reducer, which are not taken into account in the simulation, explaining discrepancies.

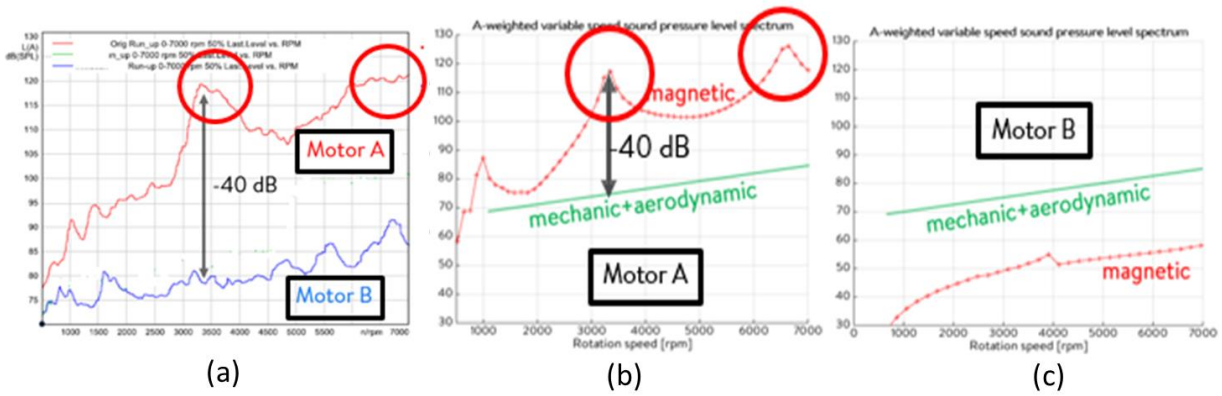

Figure 6 (a) Experimental measurements for Motor A (in red) Motor B (in green); (b) MANATEE prediction for Motor A; (c) MANATEE prediction for Motor B.

3 Vibroacoustic study of a SCIM for railway traction

3.1 Objectives

In this part, the effect of electromagnetic forces on the overall noise is studied for a SCIM of 200 kW designed for railway application, using MANATEE software. The objective is to illustrate the effect of several physical aspects that are responsible for additional noise, such as slotting and winding effects,

saturation, eccentricities, pulse-width modulation. The machine is composed of $Z_s = 36$ stator slots, $Z_r = 28$ rotor bars, and $p = 3$ pole pairs.

3.2 Sinewave response

A first simulation is processed at fixed speed $N = 1188$ RPM. Magnetic forces are computed by projecting the Maxwell stress tensor on the stator inner surface. Figure 7 illustrates the magnetic forces spatial distribution at tooth tips, for two harmonic forces at respectively 560 and 673.2 Hz, respectively of order 8 and 2.

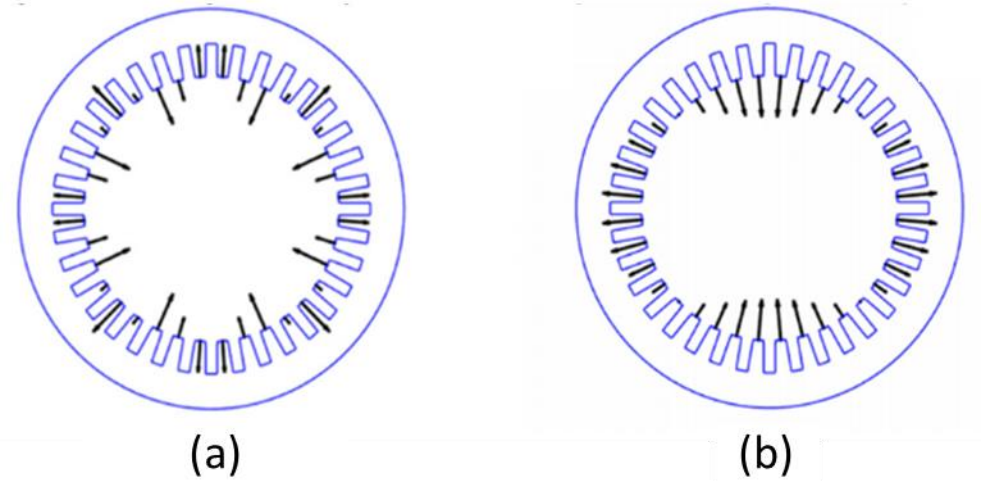

Figure 7 View of magnetic forces at tooth tips; (a) for 560 Hz; (b) for 680 Hz

Magnetic forces applied to teeth are mostly radial. In order to analyze the machine acoustic behavior, MANATEE computes the noise power level spectrum at variable speed, along with a sonogram (see Figure 8, computed within 1 second on a 2 GHz laptop). The sonogram is 2D representation of three parameters:

- On x-axis: noise pressure level frequency
- On y-axis: time or rotation speed
- On z-axis: noise pressure level magnitude

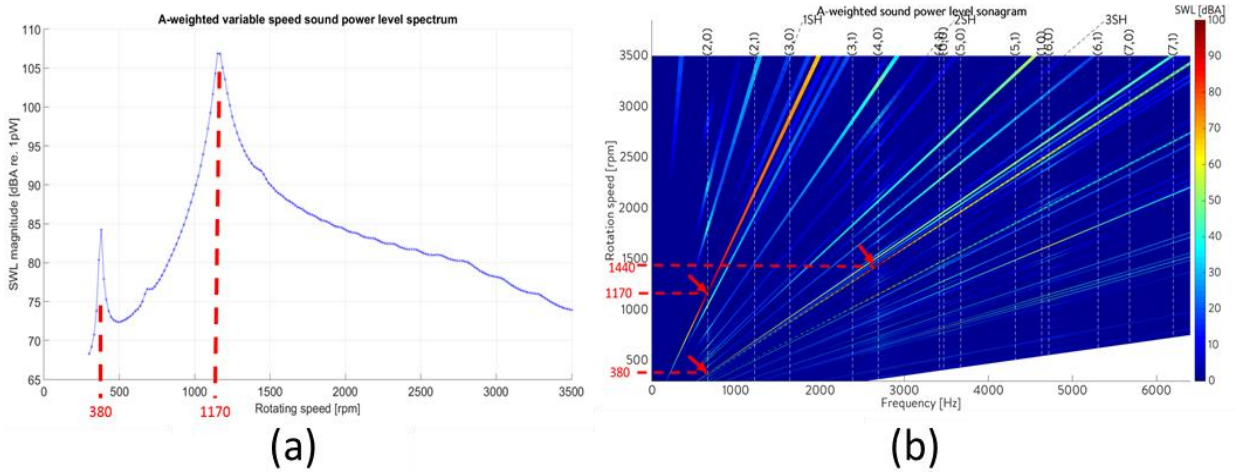

Figure 8 (a) A-weighted variable speed noise power level spectrum; (b) Sonagram of the studied machine for sinewave response

Figure 8 shows two acoustic resonances at 380 and 1188 RPM. They result from two slotting harmonics of wavenumber 2 exciting the stator oval distortion mode (2,0). A third resonance appears at 1440 RPM, and matches with the elliptic mode of wavenumber 4. All these contributions to the overall noise level can be represented as in Figure 9 using MANATEE built-in post processing tools.

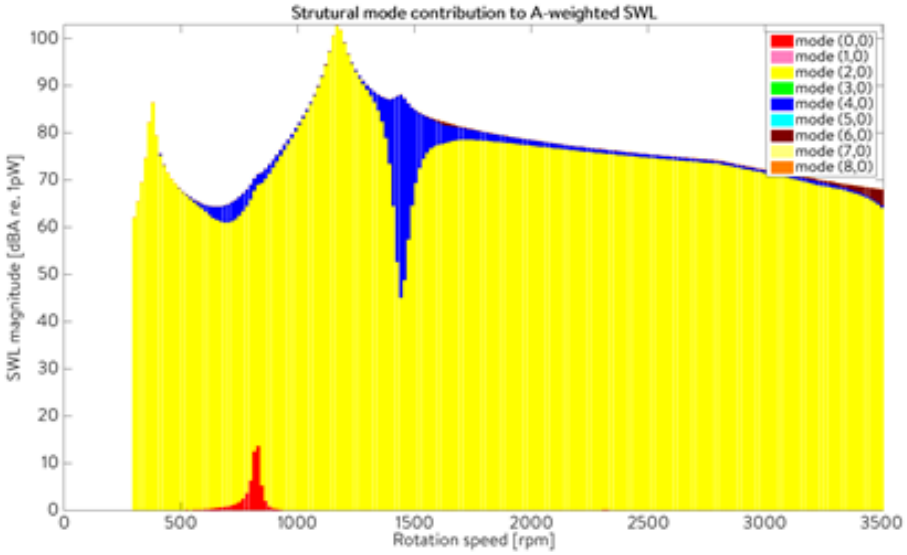

Figure 9 Modal contribution to acoustic power level

3.3 Slotting harmonics

On the studied machine, the main resonance is due to a slotting harmonic of the magnetic force. The spatial frequency expression is indeed given by $r = Z_s - Z_r - 2p = 36 - 28 - 6 = 2$, and so depends on stator and rotor tooth numbers. This wavenumber is equal to the stator oval distortion mode (2,0), which is a condition to resonance occurrence.

MANATEE software enables to process sensitivity studies in order to determine which parameters have an impact on the noise level for machine redesigning purpose. In this case, a sensitivity study is made to design a machine whose number Z_r of rotor bars minimizes the maximal acoustic power level $L_{wA,max}$ at variable speed. Results of the study are shown in Figure 10:

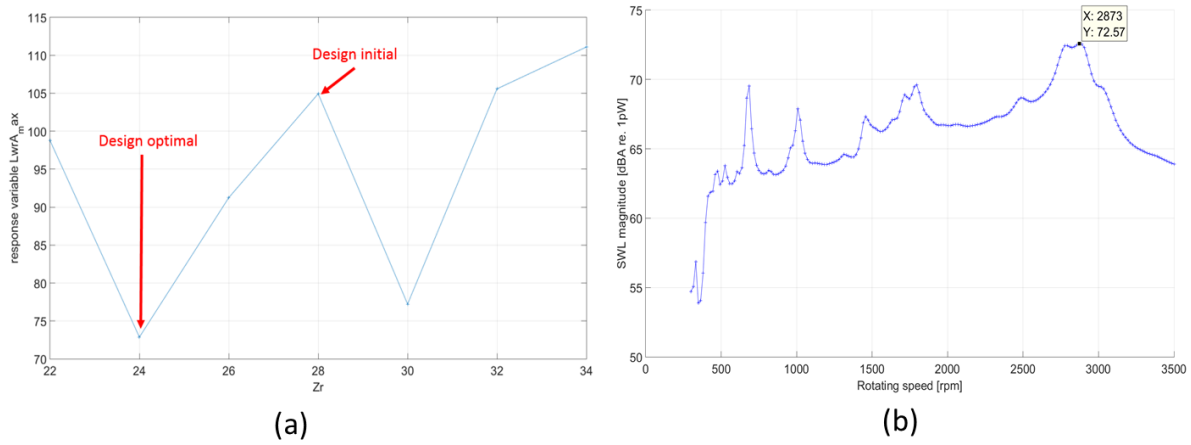

Figure 10 (a) Noise due to magnetic forces in function of the number of rotor bars ; (b) Acoustic power level in function of rotating speed for Zr=24

This graph shows that $L_{wA,max}$ is minimized for $Z_r = 24$, and so the importance of slotting harmonics in the emitted noise. Tooth numbers have a significant influence on noise power level, and which is possible to minimize by changing the topology. The sensitivity study can also include the impact of rotor slot number on electromechanical performances (ex: torque, efficiency).

3.4 Windings harmonics

Figure 11a) describes the three-phased windings distribution in the stator slots, for the studied machine. In order to analyze the effect of windings spatial distribution on noise, a different windings is simulated. The difference between both distributions is the windings pitch ratio, meaning the number of slots that each winding coil surrounds over the number of slots per pole.

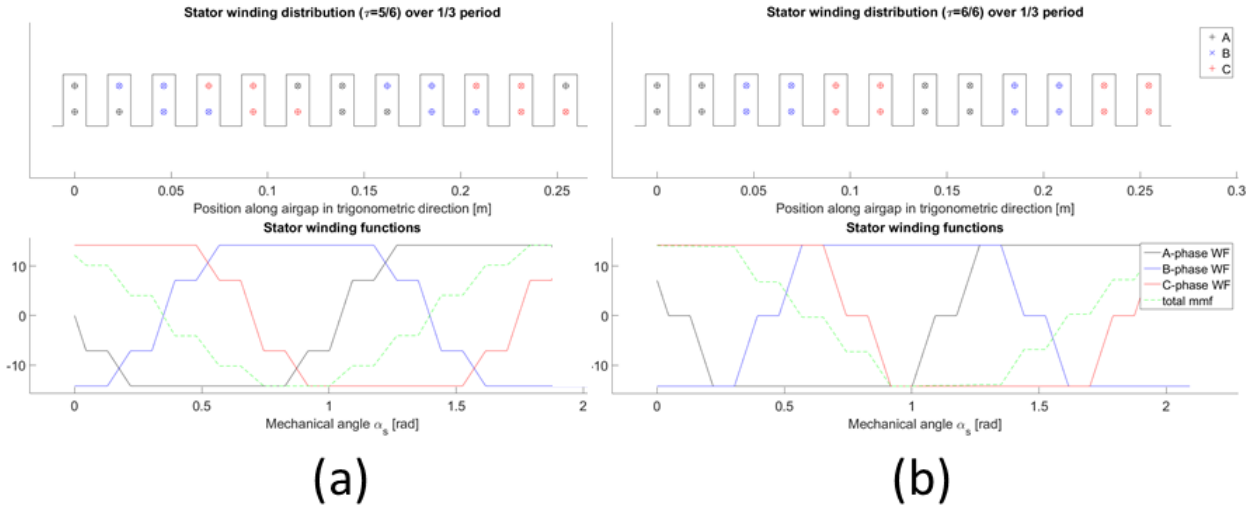

Figure 11 (a) Initial windings distribution (shorted pitch ratio: 5/6); (b) New winding distribution (without shorted pitch)

The new acoustic power level spectrum is shown in Figure 12. An additional resonance can be observed at 702 RPM, making the new winding distribution noisier. This resonance is caused by the excitation of the previously identified oval distortion mode (2,0) by a magnetic force harmonic of order $r = 2Z_s - Z_r - p - 13p = 2$, where 13p is the new stator winding harmonic component. This illustrates the effect of windings harmonics on the radiated noise.

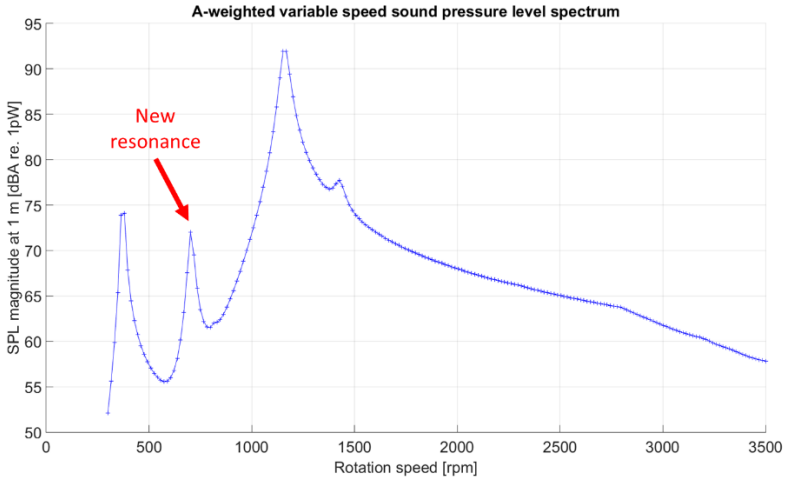

Figure 12 Effect of the winding pitch ratio

3.5 Saturation harmonics

The magnetic saturation in electrical machines is due to the non-linearity of the B(H) curve inside stator and rotor cores. To see this effect, input voltage value is twice more than the original value ($U_0 = \frac{600}{\sqrt{3}}V$). The sonogram including saturation harmonics is presented in Figure 13

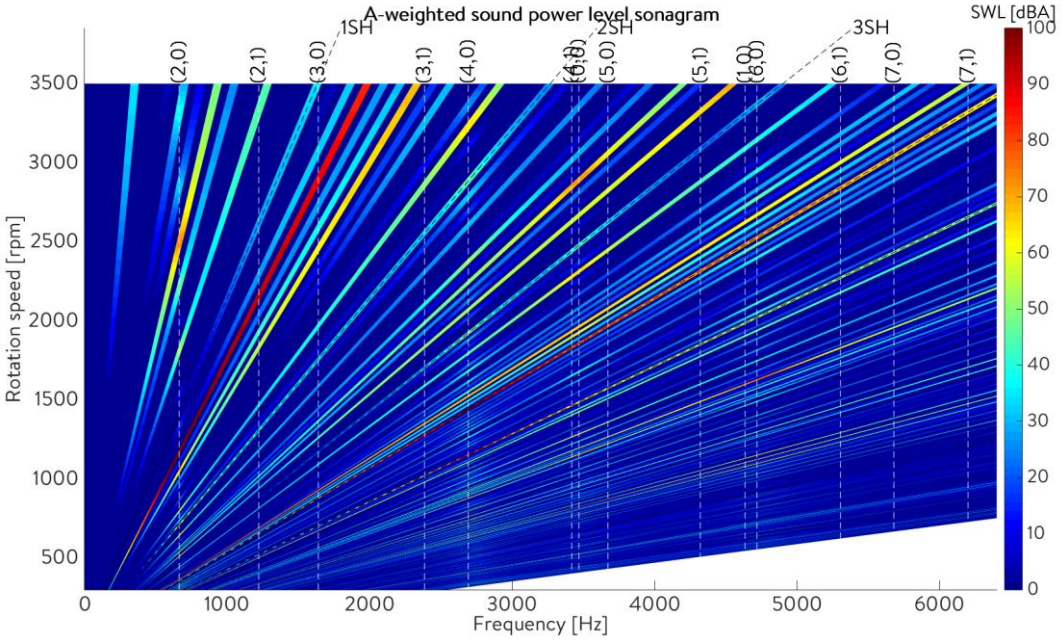

Figure 13 Sonagram of the studied machine including saturation

A new harmonic component appears near the slotting harmonic of wavenumber 2. This component due to saturation has a wavenumber expressed as $r = Z_r - Z_s + 4p = 4$ whose frequency at no-load case is $f = f_s\left(\frac{Z_r}{p}\right) + 4$. For this machine, this saturation harmonic does not create additional resonance. Yet, it could result in a high noise power level for another SCIM topology presenting structural mode of order 4.

3.6 Eccentricities harmonics

Stator and rotor should theoretically be concentric. Yet, eccentricities may appear during the assembling steps, or even as the machine is running.

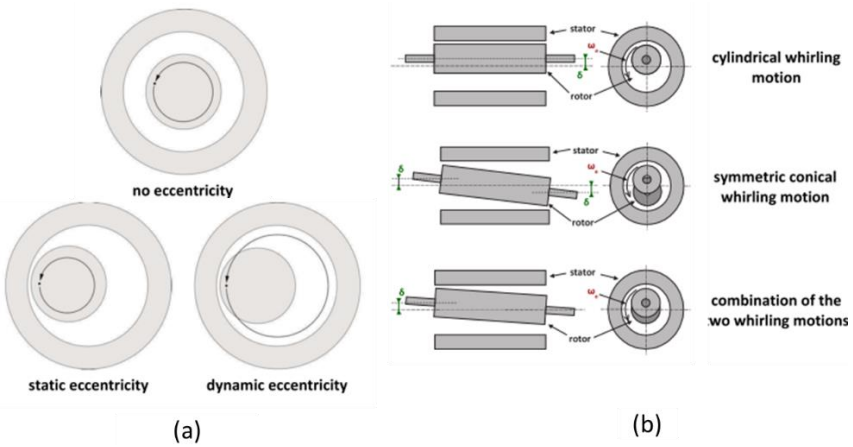

Figure 14 (a) Static and dynamic eccentricities; (b) Longitudinal whirling motions ([8][9])

MANATEE can simulate this type of fault. A 10% static eccentricity (relatively to the air gap length) is introduced. Figure 15 shows the results for the noise power level spectrum at variable speed, and the obtained sonogram.

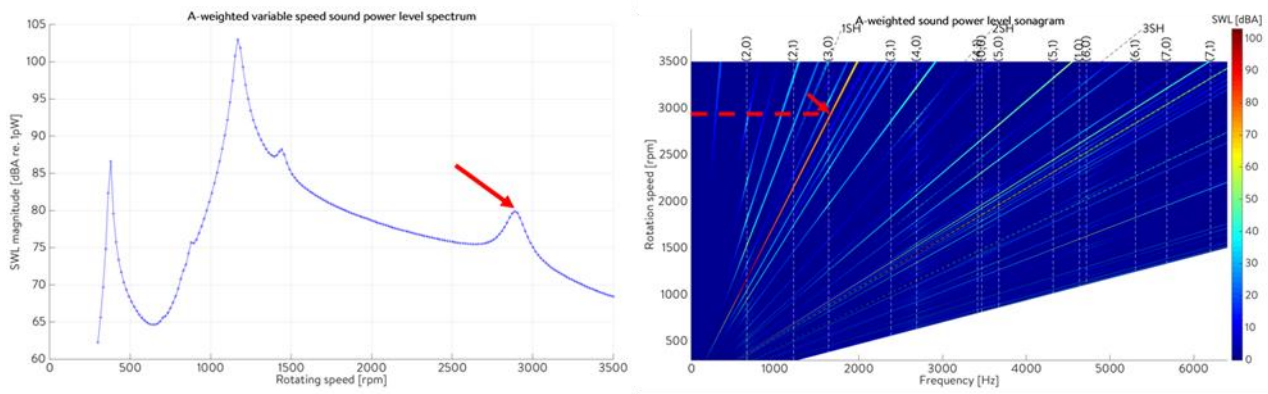

Figure 15 Study for a 10% static eccentricity: acoustic power level spectrum and sonagram

A third resonance at 2900 RPM can be observed on the spectrum. The sonogram gives insights on the eccentricity effect: the spectrum is more scattered. In fact, static eccentricity modulates each slotting harmonics order by +/-1. So, the excitation due to the slotting harmonics of wavenumber 2, which was responsible for the main resonance (see §3.3), is now duplicated in two excitations of wavenumber 1 and 3. This latter matches the structural mode (3,0), resulting in a new resonance.

A 15% dynamic eccentricity is now simulated. Figure 16 shows the results for the noise power level spectrum at variable speed, and the sonogram.

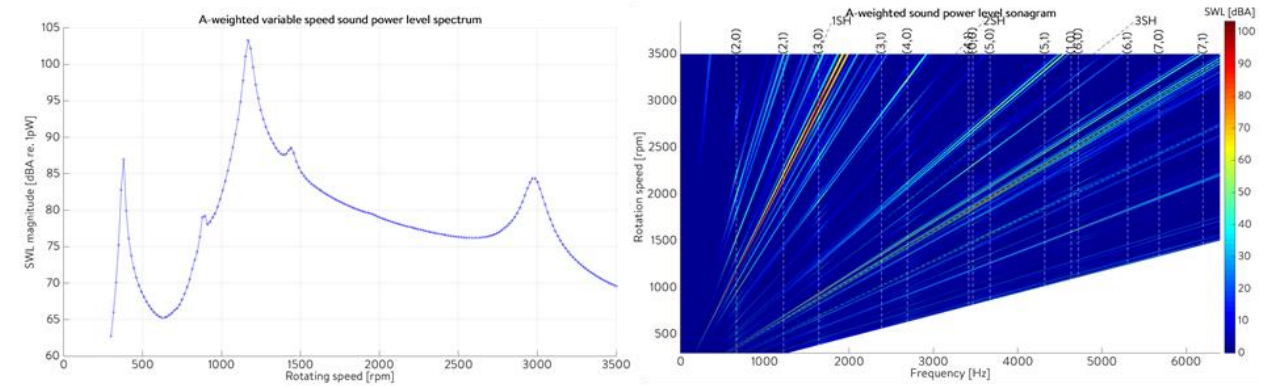

Figure 16 Study for a 15% dynamic eccentricity: acoustic power level spectrum and sonagram

As for the static eccentricity, the odd structural mode (3,0) is excited. Yet, both sonograms slightly differ: for dynamic eccentricity, the resonance peak is larger on the frequency band. This is due to the fact that dynamic eccentricity modulates the excitation both in time and spatial domains, as it was only a spatial effect for static eccentricity. This time modulation introduces side bands around the multiples of the mechanical frequency.

3.7 Airgap uneven geometry

Stator and rotor laminations may be non-circular due to segmentation effects, weldings, design constraints, mechanical deflection due to its own weight, thermal expansion etc. These singularities may also modulate magnetic forces and impact on the overall acoustic power level [10].

3.8 PWM harmonics

A PWM supply modulates magnetic forces in the time domain as consequence of the current modulation. For an asynchronous PWM, this induces "V-shape" components on the sonogram. As they do not depend on the mechanical frequency nor the fundamental supply frequency, these PWM components does not cross the sonagram origin, contrary to the other excitation components which are proportional to the fundamental frequency (slotting, windings, saturation etc.).

PWM components may excite structural modes of order 0 or 2p, or simply result in forced excitations that considerably increase the machine acoustic power level.

4 Resonance diagnosis using MANATEE

4.1 Introduction

In the previous part, magnetic noise main factors and their effects have been presented. This paragraph is dedicated to a diagnosis method which enables to retrieve the physical parameters that are responsible for a specific resonance. In particular, the objective is to understand which parameters create the excitation at 673.2Hz (see Figure 7b)) that resonates with the oval distortion mode (2,0) (Figure 8a)), at 1188 RPM, that means $f_s = 59.4\ Hz$ for the supplying fundamental frequency.

To keep this illustrative example as simple as possible, the following assumptions are made:

- The machine is at no-load state (slip is equal to 0)
- Stator and rotor cores are supposed to be non saturated,
- The rotor has no eccentricity,
- Only the fundamental frequency for power supply is considered
- The tangential component of the flux density is neglected when computing the radial pressure with the Maxwell stress tensor method.

4.2 Radial flux density and radial force computation in the air gap

The time and spatial distribution of the air gap flux density is computed using a permeance/magnetomotive force (mmf) model [5]. This analytical model is very fast and accurate to compute the radial component of the flux density, which is responsible for most of the noise in this case. The time and spatial distribution of the radial flux density as well as its FFT2D are shown in Figure 17.

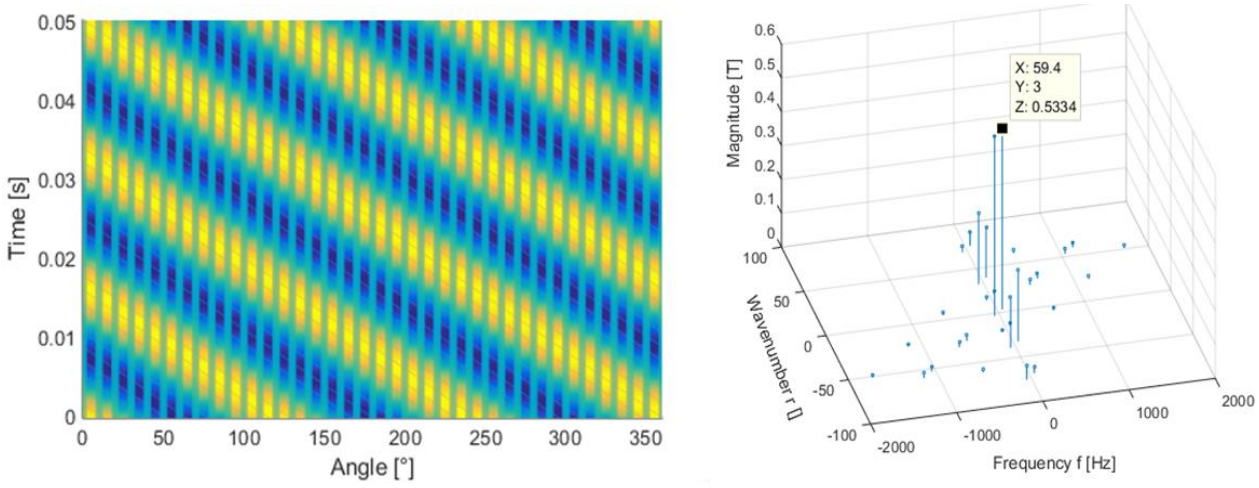

Figure 17 Spatial and time distribution of the radial flux density and its FFT2D

Magnetic forces are then deduced from the radial flux density by computing the Maxwell stress tensor at the middle of the air gap. Then, the complex FFT2D of the forces is computed and shown in Figure 18, in which the component responsible for the resonance (coincidence with the red multiplication cross) is made explicit. It is reminded that both the excitation wavenumber and frequency must match with the structural mode and frequency so that a resonance may occur.

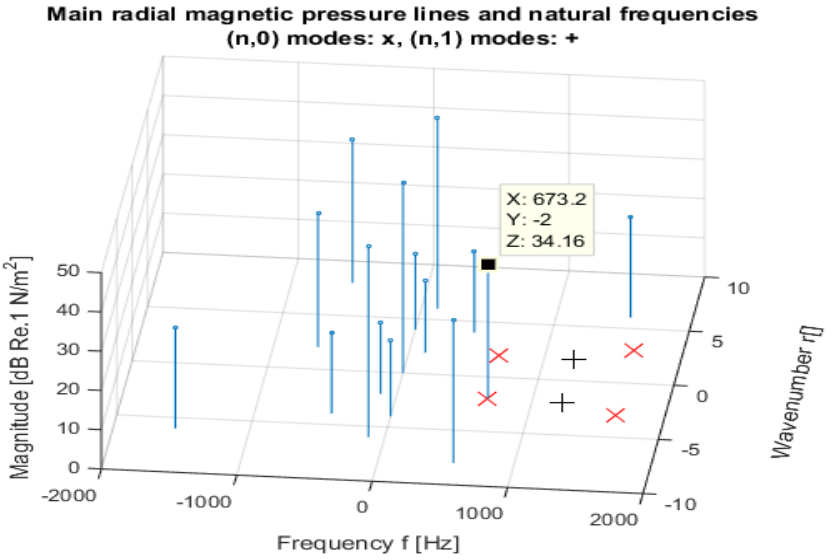

Figure 18 FFT2D of the magnetic forces with the problematic component at r=2 and f =673.2Hz

Though the excitation is identified by analyzing the FFT2D of the magnetic forces and of the flux density, it does not give insight on which the physical parameters created this excitation, hence further analysis is required.

4.3 Diagnosis the harmonics of flux density and force using convolution product method

A method based on the convolution product enables to track the origin of the components of the forces FFTD [11]. According to the Maxwell stress tensor, the time and spatial distribution of the radial pressure is equal to the square of the radial flux density. By duality with the frequency domain, it means that the force FFT2D results from the auto-convolution of the flux density FFT2D. This relation between both spectral contents enables to determine which harmonics of the flux density interact and create the exciting force of order 2 (the largest blue arrow on Figure 19).

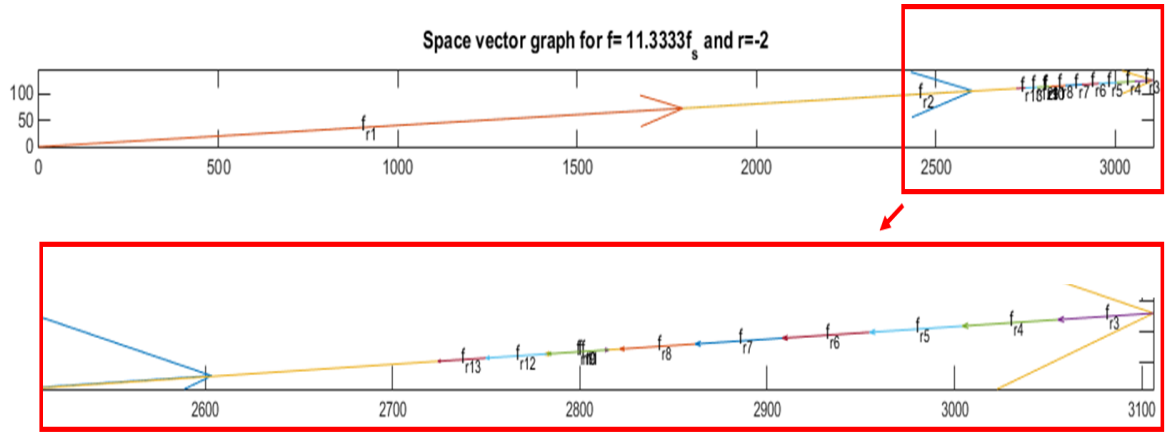

Figure 19 Vectors diagram of the flux density interaction that creates the force excitation (90% of the final force harmonic magnitude is included in the plot)

It can be seen that many flux density harmonics "B" contributes to this particular excitation f_{rtot}, by increasing or reducing its magnitude. Figure 20 gives the frequencies and the wavenumbers of the first couples of flux density components:

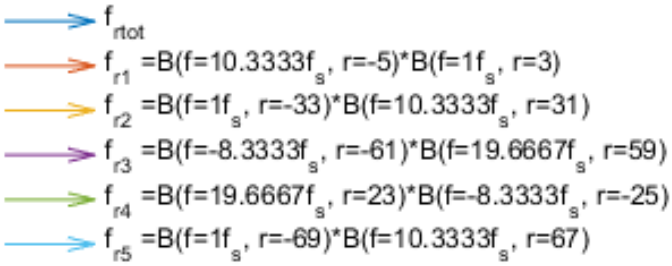

Figure 20 List of the first flux density couples creating an elementary force of order 2 at 673.2 Hz

If the flux density is computed by the permeance/mmf model, the same convolution approach enables to determine which harmonics of the permeance and of the mmf interact to create the flux density harmonics that are responsible for the excitation. For example, f_{r1} is the most important contribution to the total force and is due to the interaction of the fundamental component of the flux density ($f = f_s = 59.4Hz,\ r = p = 3$) with a higher flux density harmonic at ($f = 10.333f_s = 613.8Hz, r = -5$, with $\frac{Z_r}{p} + 1 = 10.333$). The same vectors diagram is represented in Figure 21 for this higher harmonic, giving its permeance and mmf components. This harmonic has a very small magnitude, near $8e^{-3}$ Tesla, compared to the fundamental at 0.56 Tesla.

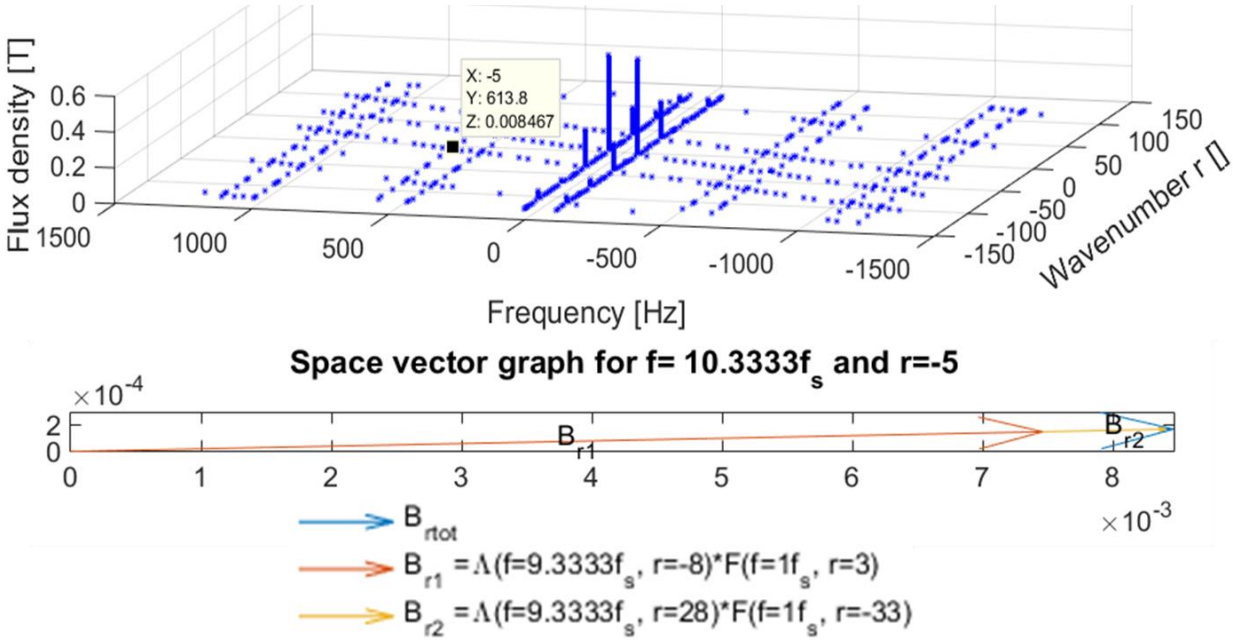

Figure 21 Permeance and mmf components of the higher flux density harmonic (f = $10.333f_s$, r=-5)

The flux density harmonic is due to two components B_{r1} and B_{r2}. The first one is due to the interaction of both stator and rotor permeances ($r = Z_r - Z_s = -8$) with the fundamental of the mmf ($r = p = 3$). The second one is due to the interaction between the 11th harmonic of the mmf ($r = -11p = -33 = -Z_s - p$) with the rotor permeance ($r = Z_r = 28$).

Based on this analysis, one can then choose the best vibration reduction method (change of the winding pitch, rotor or stator skew, optimal skew angle, etc).

5 Conclusion

Audible noise generated by electrical machines commonly used in transports (vehicles, trains, boats etc.) may be dominated by the electromagnetic noise, due to the presence of electromagnetic fields. This is the case for electrical machines used for railway tractions, whose acoustic power level due to magnetic Maxwell forces depend on the machine design (e.g.: tooth numbers, windings distribution, saturation, etc.) and control (e.g.: PWM).

Fast simulation software, such as MANATEE, enable to predict within a few seconds the impact of the design parameters on the radiated noise in the first design steps, and to diagnose noise and vibrations issues on existing electrical machines.

6 References

[1] J. Le Besnerais, P. Pellerey, V. Lanfranchi et autres, 10 nov. 2013, "*Bruit acoustique d'origine magnétique dans les machines synchrones*" dans "Machines électriques tournantes : conception, construction et commande", [en ligne], Editions T.I. [Paris, France], 2016, d3581

[2] J. Le Besnerais, V. Lanfranchi, M. Hecquet and P. Brochet, "*Characterization and Reduction of Audible Magnetic Noise Due to PWM Supply in Induction Machines*," in IEEE Transactions on Industrial Electronics, vol. 57, no. 4, pp. 1288-1295, April 2010.

[3] J. Le Besnerais, V. Lanfranchi, et M. Hecquet, et autres, 10 mai 2013, "*Bruit audible d'origine magnétique dans les machines asynchrones*" in "Machines électriques tournantes : conception, construction et commande", [en ligne], Editions T.I. [Paris, France], 2016, d3580

[4] J. Le Besnerais, "*Reduction of magnetic noise in PWM-supplied induction machines : low-noise design rules and multi-objective optimisation,*" Ph.D. dissertation, Ecole Centrale de Lille, France, Nov. 2008

[5] J. Le Besnerais, V. Lanfranchi, M. Hecquet and P. Brochet, "*Optimal Slot Numbers for Magnetic Noise Reduction in Variable-Speed Induction Motors*," in IEEE Transactions on Magnetics, vol. 45, no. 8, pp. 3131-3136, Aug. 2009.

[6] M Belahcen, "*Magnetoelasticity, magnetic forces and magnetostriction in electrical machines*" Ph.D. dissertation, Helsinki University of Technology, Finland, Aug. 2004.

[7] MANATEE software, *Magnetic Acoustic Noise Analysis Tool for Electrical Engineering*. Version 1.05, http://www.eomys.com, EOMYS ENGINEERING, 2016

[8] C. Schlensok, B. Schmülling, M. Van Der Giet, and K. Hameyer, "*Electromagnetically excited audible noise-evaluation and optimization of electrical machines by numerical simulation*", in Journal of Electrical Power Quality and Utilisation 26, 3 (2006), 727-742

[9] A. Tenhunen, T. Benedetti, T. Holopainen, and A. Arkkio, "*Electromagnetic forces in cage induction motors with rotor eccentricity*", in IEEE International Electric Machines and Drives Conference (2003), vol. 3, IEEE, pp. 1616-1622.

[10] J. Le Besnerais, "*Effect of lamination asymmetries on magnetic vibrations and acoustic noise in synchronous machines*," in 18th International Conference on Electrical Machines and Systems (ICEMS), 2015, Pattaya, 2015, pp. 1729-1733.

[11] R. Rothe, M. van der Giet, K. Hameyer, *"Convolution approach for analysis of magnetic forces in electrical machines"*, in COMPEL - The international journal for computation and mathematics in electrical and electronic engineering, 2010, Vol. 29 Iss: 6, pp.1542 - 1551